RESEARCH ARTICLE

Adaptive Tunable Predefined-Time Backstepping Control for Uncertain Robotic Manipulators

Huihui Shi[1], **Shuzong Xie**[2,*], **Qiang Chen**[1], **Shuangyi Hu**[1] **and Shenglun Yi**[3]

[1] Zhejiang University of Technology, Hangzhou 310023, China
[2] Zhejiang University of Science and Technology, Hangzhou 310023, China
[3] University of Padova, 35131 Padova, Italy

Abstract

In engineering applications, high-precision tracking control is crucial for robotic manipulators to successfully complete complex operational tasks. To achieve this goal, this study proposes an adaptive tunable predefined-time backstepping control strategy for uncertain robotic manipulators with external disturbances and model uncertainties. By establishing a novel practical predefined-time stability criterion, a tunable predefined-time backstepping controller is systematically presented, allowing the upper bound of tracking error settling time to be precisely determined by adjusting only one control parameter. To accurately address lumped uncertainty, two updating laws are designed: a fuzzy weight updating law and a boundary adaptive updating law, which together reduce dependence on system model knowledge. In addition, the singularity problem in the predefined-time design process is effectively avoided by constructing the hyperbolic tangent function. The efficacy of the proposed control strategy is verified through numerical simulations.

Keywords: predefined-time control, adaptive fuzzy control, backstepping design, robotic manipulators.

1 Introduction

Over the past few decades, robotic manipulators have been widely applied in various industries such as manufacturing, material handling, and space exploration, significantly enhancing automation levels and work efficiency [1, 2]. However, in practical operations, robotic manipulators inevitably face external disturbances and model uncertainties, which pose severe challenges for achieving high-speed and high-precision tracking control. To this end, researchers have proposed various advanced control strategies, including learning control [3–5], sliding mode control (SMC) [6], model predictive control (MPC) [7], adaptive fuzzy/neural control [8–10], and so on. Unfortunately, these control strategies [3–10] can only achieve asymptotic convergence of position tracking errors, meaning that the convergence time for the errors is infinite, making it difficult to meet tasks with strict convergence time requirements.

To achieve satisfactory tracking performance for robotic manipulators, finite-time control [11–13] and

Academic Editor:
Aradhana Misra

Submitted: 17 October 2024
Accepted: 05 December 2024
Published: 18 December 2024

Vol. 1, **No.** 2, 2024.
10.62762/TSCC.2024.672831

***Corresponding author:**
Shuzong Xie
xieshuzong@zust.edu.cn

Citation
Shi, H., Xie, S., Chen, Q., Hu, S., & Yi, S. (2024). Adaptive Tunable Predefined-Time Backstepping Control for Uncertain Robotic Manipulators. *ICCK Transactions on Sensing, Communication, and Control*, 1(2), 126–135.

fixed-time control [14–16] have been proposed and quickly developed due to its outstanding performance with respect to rapid convergence rate and high control accuracy. In [13], a composite learning controller was designed based on a nonsingular terminal sliding mode surface, enabling tracking and estimation errors to converge to zero in finite time. Van et al. [16] investigated the fixed-time backstepping tracking control problem to ensure the fixed-time convergence of tracking errors. However, finite/fixed-time control (e.g., [11–16]) has the following two limitations: (i) the convergence time is highly dependent on the system's initial conditions, meaning that a larger initial value results in a longer convergence time; (ii) the convergence time is a complex function of multiple control parameters, making it difficult to establish a direct relationship between convergence time and control parameters. For example, in automated assembly lines or precision assembly tasks, robotic manipulators need to accurately reach the target position within the expected time to ensure the correct assembly and alignment of components.

To address the limitations of finite/fixed-time control, the concept of predefined-time stability was first proposed in [17], offering the key advantage of precisely determining the upper bound of convergence time by adjusting only one control parameter. With this advantage, researchers have successfully applied predefined-time control to various nonlinear systems [18–24]. However, there are mainly two issues in the previous predefined-time control literature: (i) an overestimation of the upper bound of the convergence time, i.e., $\sqrt{2}T_c$ or $2T_c$, with T_c being a predefined-time constant [18–21]; (ii) the introduction of some piecewise continuous functions to address the controller singularity problem increases the complexity of stability analysis [22–24]. More recently, scholars presented several predefined-time criteria with the upper bound of the convergence time being T_c instead of $\sqrt{2}T_c$ or $2T_c$, which is beneficial for practical applications [25, 26]. In [26], a predefined-time robust stabilization strategy was proposed for robotic manipulators, where the singularity problem was not considered, and robust approach was adopted to suppress system uncertainties. Thus, designing a singularity-free predefined-time control strategy to avoid overestimating the upper bound of the convergence time for tracking error is both challenging and meaningful.

Based on above discussions, an adaptive tunable predefined-time backstepping tracking control strategy is proposed for robotic manipulators with external disturbances and model uncertainties, and the main contributions are listed as follows.

(i) Compared to finite/fixed-time control [11, 13–16], a tunable predefined-time controller is devised by establishing a novel practical predefined-time stability criterion, ensuring that the upper bound of convergence time of tracking errors can be precisely determined by adjusting only one control parameter.

(ii) By constructing a fuzzy weight updating law and a boundary adaptive updating law, the knowledge of lumped uncertainty including external disturbances, model uncertainties, and fuzzy approximation errors, is no longer required. Moreover, the singularity problem in the controller can be directly avoided by constructing the hyperbolic tangent function.

The remainder of this study is organized as follows: Section II outlines the dynamic model of the robotic manipulator system and some essential lemmas. Section III provides the predefined-time control design process and stability analysis. The simulation results arevalidated in Section IV. Finally, followed by conclusions in Section V.

2 Problem Formulation and Preliminaries

2.1 Dynamic model of robotic manipulators

The dynamic model of the n-DOF robotic manipulator system can be described as [26]

$$\boldsymbol{M}(\boldsymbol{q})\ddot{\boldsymbol{q}} + \boldsymbol{C}(\boldsymbol{q},\dot{\boldsymbol{q}})\dot{\boldsymbol{q}} + \boldsymbol{G}(\boldsymbol{q}) = \boldsymbol{u} + \boldsymbol{d} \tag{1}$$

where $\boldsymbol{q},\dot{\boldsymbol{q}},\ddot{\boldsymbol{q}} \in \Re^n$, $\boldsymbol{M}(\boldsymbol{q}) \in \Re^{n\times n}$, $\boldsymbol{C}(\boldsymbol{q},\dot{\boldsymbol{q}}) \in \Re^{n\times n}$, $\boldsymbol{G}(\boldsymbol{q}) \in \Re^n$, $\boldsymbol{M}(\boldsymbol{q}) = \boldsymbol{M}_0(\boldsymbol{q}) + \Delta\boldsymbol{M}(\boldsymbol{q})$, $\boldsymbol{C}(\boldsymbol{q},\dot{\boldsymbol{q}}) = \boldsymbol{C}_0(\boldsymbol{q},\dot{\boldsymbol{q}}) + \Delta\boldsymbol{C}(\boldsymbol{q},\dot{\boldsymbol{q}})$, $\boldsymbol{G}(\boldsymbol{q}) = \boldsymbol{G}_0(\boldsymbol{q}) + \Delta\boldsymbol{G}(\boldsymbol{q})$, $\boldsymbol{d} \in \Re^n$, $\boldsymbol{u} \in \Re^n$, and the corresponding definitions of these symbols are given in Table 1.

By defining $\boldsymbol{x}_1 = \boldsymbol{q}$ and $\boldsymbol{x}_2 = \dot{\boldsymbol{q}}$, the dynamic model of robotic manipulator system (1) can be rewritten as

$$\begin{cases} \dot{\boldsymbol{x}}_1 = \boldsymbol{x}_2 \\ \dot{\boldsymbol{x}}_2 = \boldsymbol{F} + \boldsymbol{\Upsilon} + \boldsymbol{M}_0^{-1}(\boldsymbol{x}_1)\boldsymbol{u} + \boldsymbol{D} \end{cases} \tag{2}$$

where $\boldsymbol{F} = -\boldsymbol{M}_0^{-1}\big(\boldsymbol{C}_0(\boldsymbol{x}_1,\boldsymbol{x}_2)\boldsymbol{x}_2 + \boldsymbol{G}_0(\boldsymbol{x}_1)\big)$, $\boldsymbol{\Upsilon} = -\boldsymbol{M}_0^{-1}\big(\Delta\boldsymbol{C}(\boldsymbol{x}_1,\boldsymbol{x}_2)\boldsymbol{x}_2 + \Delta\boldsymbol{G}(\boldsymbol{x}_1) + \Delta\boldsymbol{M}\dot{\boldsymbol{x}}_2\big)$, and $\boldsymbol{D} = \boldsymbol{M}_0^{-1}\boldsymbol{d}$.

The control objective of this study is to design an adaptive tunable predefined-time backstepping controller for uncertain robotic manipulators with external disturbances and model uncertainties, such

Table 1. Definitions of symbols in robotic manipulators.

Symbol	Definition
$\boldsymbol{q}$	the joint position
$\dot{\boldsymbol{q}}$	the joint velocity
$\ddot{\boldsymbol{q}}$	the joint acceleration
$\boldsymbol{M}(\boldsymbol{q})$	the positive definite inertia matrix
$\boldsymbol{M}_0(\boldsymbol{q})$	the nominal part of $\boldsymbol{M}(\boldsymbol{q})$
$\Delta\boldsymbol{M}(\boldsymbol{q})$	the uncertain part of $\boldsymbol{M}(\boldsymbol{q})$
$\boldsymbol{C}(\boldsymbol{q},\dot{\boldsymbol{q}})$	the Coriolis/centrifugal torque
$\boldsymbol{C}_0(\boldsymbol{q},\dot{\boldsymbol{q}})$	the nominal part of $\boldsymbol{C}(\boldsymbol{q},\dot{\boldsymbol{q}})$
$\Delta\boldsymbol{C}(\boldsymbol{q},\dot{\boldsymbol{q}})$	the uncertain part of $\boldsymbol{C}(\boldsymbol{q},\dot{\boldsymbol{q}})$
$\boldsymbol{G}(\boldsymbol{q})$	the gravity torque
$\boldsymbol{G}_0(\boldsymbol{q})$	the nominal part of $\boldsymbol{G}(\boldsymbol{q})$
$\Delta\boldsymbol{G}(\boldsymbol{q})$	the uncertain part of $\boldsymbol{G}(\boldsymbol{q})$
$\boldsymbol{d}$	the bounded external disturbance
$\boldsymbol{u}$	the control torque

that the joint position $\boldsymbol{q}$ can rapidly and accuracyly track its desired trajectory $\boldsymbol{q}_d$, i.e., the tracking error $\boldsymbol{e}=\boldsymbol{q}-\boldsymbol{q}_d$ can converge to a sufficiently small region around the origin within the predefined time T_s.

Assumption 1 [27] *The desired joint position trajectory $\boldsymbol{q}_d$, and its first-order derivative $\dot{\boldsymbol{q}}_d$ and second-order derivative $\ddot{\boldsymbol{q}}_d$ are assumed to be continuous and bounded.*

Remark 1 *In practice, obtaining an accurate dynamic model of the robotic manipulator is quite challenging due to factors such as significant flexibility, coulomb friction, wear, and other influences. To improve the accuracy of modeling, this study separates the model into nominal and uncertain parts, i.e., $\boldsymbol{M}(\boldsymbol{q})=\boldsymbol{M}_0(\boldsymbol{q})+\Delta\boldsymbol{M}(\boldsymbol{q})$, $\boldsymbol{C}(\boldsymbol{q},\dot{\boldsymbol{q}})=\boldsymbol{C}_0(\boldsymbol{q},\dot{\boldsymbol{q}})+\Delta\boldsymbol{C}(\boldsymbol{q},\dot{\boldsymbol{q}})$, and $\boldsymbol{G}(\boldsymbol{q})=\boldsymbol{G}_0(\boldsymbol{q})+\Delta\boldsymbol{G}(\boldsymbol{q})$.*

Remark 2 *From the perspective of practical engineering, the joint position $\boldsymbol{q}$, the joint velocity $\dot{\boldsymbol{q}}$ and the joint acceleration $\ddot{\boldsymbol{q}}$ are bounded due to the mechanic limitations or the task space limitations of the space manipulator [28]. Moreover, the external disturbance $\boldsymbol{d}$ is bounded, and $\boldsymbol{M}(\boldsymbol{q})$, $\boldsymbol{C}(\boldsymbol{q},\dot{\boldsymbol{q}})$, $\boldsymbol{G}(\boldsymbol{q})$ are continuous functions of the coordinates $\boldsymbol{q}$ and $\dot{\boldsymbol{q}}$. Thus, it is reasonable to assume that $\boldsymbol{\Upsilon}$ and $\boldsymbol{D}$ are bounded.*

2.2 Preliminaries

For the convenience of controller design, we first provide the following essential lemmas.

Lemma 1 *For the nonlinear system $\dot{\boldsymbol{x}}=\boldsymbol{f}(t,\boldsymbol{x})$, consider a positive definite function $V(\boldsymbol{x})$ and the scalars $\beta_1>0,\beta_2>0,\kappa>0,b>1,0<\gamma<1,T_s>0$, and $0<\vartheta<\infty$, which satisfy the following condition*

$$\dot{V}(\boldsymbol{x})\leq-\frac{b\pi}{\kappa\gamma T_s\sqrt{\beta_1\beta_2}}\left(\beta_1V^{1-\frac{\gamma}{2}}(\boldsymbol{x})+\beta_2\kappa^2V^{1+\frac{\gamma}{2}}(\boldsymbol{x})\right)+\vartheta, \tag{3}$$

and the trajectory of $\dot{\boldsymbol{x}}=\boldsymbol{f}(t,\boldsymbol{x})$ is practical tunable predefined-time stable (PTPTS), with the convergence region being

$$\left\{\lim_{t\to T_s}\boldsymbol{x}\mid V(\boldsymbol{x})\leq\min\left\{\left(\frac{b\vartheta\kappa\gamma T_s}{(b^2-1)\pi}\sqrt{\frac{\beta_2}{\beta_1}}\right)^{\frac{2}{2-\gamma}},\left(\frac{b\vartheta\kappa\gamma T_s}{(b^2-1)\pi}\sqrt{\frac{\beta_1}{\beta_2}}\right)^{\frac{2}{2+\gamma}}\right\}\right\} \tag{4}$$

where T_s is the predefined-time constant.

Proof The inequality (3) includes the following two cases, i.e.,

Case I:

$$\begin{aligned}\dot{V}(\boldsymbol{x})\leq&-\frac{b\pi}{\kappa\gamma T_s\sqrt{\beta_1\beta_2}}\left[\frac{\beta_1}{b^2}V^{1-\frac{\gamma}{2}}(\boldsymbol{x})+\beta_2\kappa^2V^{1+\frac{\gamma}{2}}(\boldsymbol{x})\right]\\&-\frac{b\pi}{\kappa\gamma T_s\sqrt{\beta_1\beta_2}}\left[(1-\frac{1}{b^2})\beta_1V^{1-\frac{\gamma}{2}}(\boldsymbol{x})\right]+\vartheta.\end{aligned} \tag{5}$$

According to (5), the following inequality

$$\dot{V}(\boldsymbol{x})\leq-\frac{b\pi}{\kappa\gamma T_s\sqrt{\beta_1\beta_2}}\left[\frac{\beta_1}{b^2}V^{1-\frac{\gamma}{2}}(\boldsymbol{x})+\beta_2\kappa^2V^{1+\frac{\gamma}{2}}(\boldsymbol{x})\right] \tag{6}$$

holds for $V^{1-\frac{\gamma}{2}}(\boldsymbol{x})\geq\frac{b\vartheta\kappa\gamma T_s}{(b^2-1)\pi}\sqrt{\frac{\beta_2}{\beta_1}}$, which can be deduced that the convergence region is $\Delta_1=\left\{\boldsymbol{x}|V(\boldsymbol{x})\leq\left(\frac{b\vartheta\kappa\gamma T_s}{(b^2-1)\pi}\sqrt{\frac{\beta_2}{\beta_1}}\right)^{\frac{2}{2-\gamma}}\right\}$.

From the inequality (6), the settling-time function can be calculated as

$$\begin{aligned}T(\boldsymbol{x}_0)\leq&-\int_{V(\boldsymbol{x}_0)}^{0}\frac{dV(\boldsymbol{x})}{\frac{b\pi}{\kappa\gamma T_s\sqrt{\beta_1\beta_2}}\left[\frac{\beta_1}{b^2}V^{1-\frac{\gamma}{2}}(\boldsymbol{x})+\beta_2\kappa^2V^{1+\frac{\gamma}{2}}(\boldsymbol{x})\right]}\\\leq&\frac{2T_s}{\pi}\int_0^{V(\boldsymbol{x}_0)}\frac{1}{1+\frac{\beta_2}{\beta_1}\kappa^2b^2V^{\gamma}(\boldsymbol{x})}d\left(\sqrt{\frac{\beta_2}{\beta_1}}\kappa bV^{\frac{\gamma}{2}}(\boldsymbol{x})\right)\\=&\frac{2T_s}{\pi}\left[\arctan\left(\sqrt{\frac{\beta_2}{\beta_1}}\kappa bV^{\frac{\gamma}{2}}(\boldsymbol{x}_0)\right)\right]\end{aligned} \tag{7}$$

Due to the fact that $\boldsymbol{x}_0$ is the initial state, $0<\arctan\left(\sqrt{\frac{\beta_2}{\beta_1}}\kappa bV^{\frac{\gamma}{2}}(\boldsymbol{x}_0)\right)\leq\frac{\pi}{2}$ is ensured. Thus, the settling time is bounded by $T(\boldsymbol{x}_0)\leq T_s$.

Case II:

$$\dot{V}(\boldsymbol{x}) \leq -\frac{b\pi}{\kappa\gamma T_s\sqrt{\beta_1\beta_2}}\left[\beta_1 V^{1-\frac{\gamma}{2}}(\boldsymbol{x})+\frac{\beta_2\kappa^2}{b^2}V^{1+\frac{\gamma}{2}}(\boldsymbol{x})\right] -\frac{b\pi}{\kappa\gamma T_s\sqrt{\beta_1\beta_2}}\left[(1-\frac{1}{b^2})\beta_2\kappa^2 V^{1+\frac{\gamma}{2}}(\boldsymbol{x})\right]+\vartheta. \tag{8}$$

Similar to the proof procedures in Case 1, the convergence region and the upper-bound settling time of the system are given by $\Delta_2 = \left\{\lim_{t\to T_s}\boldsymbol{x}|V(\boldsymbol{x}) \leq \left(\frac{b\vartheta\kappa\gamma T_s}{(b^2-1)\pi}\sqrt{\frac{\beta_1}{\beta_2}}\right)^{\frac{2}{2+\gamma}}\right\}$ and $T(\boldsymbol{x}_0)\leq T_s$, respectively.

Lemma 2 [29] *For $x\in\Re$ and $\epsilon>0$, the following inequality is satisfied*

$$0\leq|x|-x\tanh\left(\frac{x}{\epsilon}\right)\leq 0.2785\epsilon. \tag{9}$$

Lemma 3 [20] *For $x\in\Re$, $y\in\Re$, and $o_1>0, o_2>0, \delta>0$, the following relationship holds*

$$|x|^{o_1}|y|^{o_2}\leq\frac{o_1}{o_1+o_2}\delta|x|^{o_1+o_2}+\frac{o_2}{o_1+o_2}\delta^{-\frac{o_1}{o_2}}|y|^{o_1+o_2}. \tag{10}$$

Lemma 4 [30] *For $y\geq x$, and $\gamma>1$, one can obtain*

$$x(y-x)^{\gamma}\leq\frac{\gamma}{1+\gamma}(y^{1+\gamma}-x^{1+\gamma}). \tag{11}$$

Lemma 5 [31] *For $\chi_i>0, i=1,2,...,n$, and $\gamma>0$, the following inequalities hold*

$$\begin{cases}\sum_{i=1}^{n}\chi_i^{\gamma}\geq\left(\sum_{i=1}^{n}\chi_i\right)^{\gamma}, & \text{if}\quad 0<\gamma<1\\ \sum_{i=1}^{n}\chi_i^{\gamma}\geq n^{1-\gamma}\left(\sum_{i=1}^{n}\chi_i\right)^{\gamma}, & \text{if}\quad \gamma>1.\end{cases} \tag{12}$$

3 Adaptive Tunable Predefined-Time Control

In this section, an adaptive tunable predefined-time controller is developed for the robotic manipulator system (2) using the backstepping technique, followed by the predefined-time stability analysis.

3.1 Controller Design

Step 1: Select the following Lyapunov function as

$$V_1=\frac{1}{2}\boldsymbol{e}^{\mathrm{T}}\boldsymbol{e} \tag{13}$$

where $\boldsymbol{e}=[e_1,...,e_n]^{\mathrm{T}}$.

Differentiating (13) yields

$$\begin{aligned}\dot{V}_1=&\boldsymbol{e}^{\mathrm{T}}\dot{\boldsymbol{e}}\\ =&\boldsymbol{e}^{\mathrm{T}}\boldsymbol{z}+\boldsymbol{e}^{\mathrm{T}}\boldsymbol{\alpha}\end{aligned} \tag{14}$$

where $\boldsymbol{z}=[z_1,...,z_n]^{\mathrm{T}}=\dot{\boldsymbol{e}}-\boldsymbol{\alpha}$ is the virtual error, and $\boldsymbol{\alpha}=[\alpha_1,...,\alpha_n]^{\mathrm{T}}$ is the virtual controller given by

$$\alpha_i=-\bar{\alpha}_i\tanh\left(\frac{e_i\bar{\alpha}_i}{\varpi}\right) \tag{15}$$

$$\bar{\alpha}_i=k_1\mathrm{sig}^{1-\gamma}(e_i)+k_2\mathrm{sig}^{1+\gamma}(e_i)+k_3e_i \tag{16}$$

where $k_1=\bar{k}_1(\frac{1}{2})^{1-\frac{\gamma}{2}}$, $\bar{k}_1=\frac{b\pi}{\kappa\gamma T_s}\sqrt{\frac{\beta_1}{\beta_2}}$, $k_2=\bar{k}_2(\frac{1}{2})^{1+\frac{\gamma}{2}}$, $\bar{k}_2=n^{\frac{\gamma}{2}}2^{\frac{\gamma}{2}}3^{\frac{\gamma}{2}}\frac{b\pi\kappa}{\gamma T_s}\sqrt{\frac{\beta_2}{\beta_1}}$, $k_3\geq\frac{1}{2}$, $T_s>0, 0<\gamma<1, \varpi>0, \beta_1>0, \beta_2>0, \kappa>0, b>1, \mathrm{sig}^{\gamma}(\cdot)=|\cdot|^{\gamma}\mathrm{sign}(\cdot)$ with $\mathrm{sign}(\cdot)$ being the signum function, and $i=1,2,...,n$.

Differentiating (16) yields

$$\begin{aligned}\dot{\alpha}_i=&-\dot{\bar{\alpha}}_i\tanh\left(\frac{e_i\bar{\alpha}_i}{\varpi}\right)-\bar{\alpha}_i\left(1-\tanh^2\left(\frac{e_i\bar{\alpha}_i}{\varpi}\right)\right)\cdot\\ &\frac{1}{\varpi}(\dot{e}_i\bar{\alpha}_i+e_i\dot{\bar{\alpha}}_i)\end{aligned} \tag{17}$$

where $\dot{\bar{\alpha}}_i$ is calculated as

$$\dot{\bar{\alpha}}_i=k_1(1-\gamma)|e_i|^{-\gamma}\dot{e}_i+k_2(1+\gamma)|e_i|^{\gamma}\dot{e}_i+k_3\dot{e}_i \tag{18}$$

From (15)-(18), it can be obtained that when $e_i=0, \dot{e}_i\neq 0$, the term $\dot{\bar{\alpha}}_i\tanh\left(\frac{e_i\bar{\alpha}_i}{\varpi}\right)=0$ and the power of the term $e_i\dot{\bar{\alpha}}_i = k_1(1-\gamma)\mathrm{sig}^{1-\gamma}(e_i)\dot{e}_i+k_2(1+\gamma)\mathrm{sig}^{1+\gamma}(e_i)\dot{e}_i+k_3e_i\dot{e}_i$ is positive. Thus, the singularity problem cuased by the differentiation of conventional vitural control $\dot{\bar{\alpha}}_i$ can be directly avoided.

According Lemma 2, one has

$$\begin{aligned}e_i\alpha_i=&-e_i\bar{\alpha}_i\tanh\left(\frac{e_i\bar{\alpha}_i}{\varpi}\right)\\ \leq&-e_i\bar{\alpha}_i+0.2785\varpi\end{aligned} \tag{19}$$

further implies that

$$\boldsymbol{e}^{\mathrm{T}}\boldsymbol{\alpha}\leq-\boldsymbol{e}^{\mathrm{T}}\bar{\boldsymbol{\alpha}}+0.2785n\varpi \tag{20}$$

where $\bar{\boldsymbol{\alpha}}=[\bar{\alpha}_1,...,\bar{\alpha}_n]^{\mathrm{T}}$.

Substituting (15), (16), (20) into (14) and using Lemma 5, one can obtain

$$\begin{aligned}\dot{V}_1\leq&\boldsymbol{e}^{\mathrm{T}}\boldsymbol{z}-\boldsymbol{e}^{\mathrm{T}}\bar{\boldsymbol{\alpha}}+0.2785n\varpi\\ \leq&\frac{||\boldsymbol{e}||^2}{2}+\frac{||\boldsymbol{z}||^2}{2}-k_1(||\boldsymbol{e}||^2)^{1-\frac{\gamma}{2}}-k_2(||\boldsymbol{e}||^2)^{1+\frac{\gamma}{2}}-\\ &k_3||\boldsymbol{e}||^2+0.2785n\varpi\\ \leq&-\bar{k}_1V_1^{1-\frac{\gamma}{2}}-\bar{k}_2n^{-\frac{\gamma}{2}}V_1^{1+\frac{\gamma}{2}}+0.2785n\varpi+\frac{||\boldsymbol{z}||^2}{2}\end{aligned} \tag{21}$$

Step 2: Define the Lyapunov function as follows

$$V_2 = V_1 + \frac{1}{2}\boldsymbol{z}^{\mathrm{T}}\boldsymbol{z}. \tag{22}$$

Differentiating (22) results in

$$\begin{aligned}\dot{V}_2 =&\dot{V}_1 + \boldsymbol{z}^{\mathrm{T}}(\ddot{\boldsymbol{e}} - \dot{\boldsymbol{\alpha}})\\ =&\dot{V}_1 + \boldsymbol{z}^{\mathrm{T}}\left[\boldsymbol{F} + \boldsymbol{\Lambda} + \boldsymbol{M}_0^{-1}\boldsymbol{u} + \boldsymbol{D} - \ddot{\boldsymbol{q}}_d\right]\end{aligned} \tag{23}$$

where the uncertainty $\boldsymbol{\Lambda} = [\Lambda_1, ..., \Lambda_n]^{\mathrm{T}} = \boldsymbol{\Upsilon} - \dot{\boldsymbol{\alpha}}$ can be approximated using the fuzzy logic systems (FLSs) [32], i.e.,

$$\Lambda_i = \boldsymbol{W}_i{}^{\mathrm{T}}\boldsymbol{S}_i(\boldsymbol{X}_n) + \varepsilon_i, i = 1, 2, ..., n \tag{24}$$

where $\boldsymbol{X}_n = [\boldsymbol{x}_1^{\mathrm{T}}, \boldsymbol{x}_2^{\mathrm{T}}, \boldsymbol{e}^{\mathrm{T}}]^{\mathrm{T}}$ denotes the input vector, ε_i represents the approximation error satisfying $|\varepsilon_i| \leq \varepsilon_N$ with ε_N being a positive constant, $\boldsymbol{W}_i$ and $\boldsymbol{S}_i$ are the weight vector and the basis function of FLSs, respectively.

Substituting (24) into (23) yields

$$\dot{V}_2 = \dot{V}_1 + \sum_{i=1}^{n} z_i\boldsymbol{W}_i^{\mathrm{T}}\boldsymbol{S}_i + \boldsymbol{z}^{\mathrm{T}}\left[\boldsymbol{F} + \boldsymbol{D}' + \boldsymbol{M}_0^{-1}\boldsymbol{u} - \ddot{\boldsymbol{q}}_d\right] \tag{25}$$

where $\boldsymbol{D}' = [D_1', ..., D_n']^{\mathrm{T}} = \varepsilon + \boldsymbol{D}$ is the composite disturbance, and there is an unknown positive constant d_a, such that $||\boldsymbol{D}'|| \leq d_a$.

Subsequently, the predefined-time controller $\boldsymbol{u} = [u_1, ..., u_n]^{\mathrm{T}}$ is designed as

$$\begin{aligned}\boldsymbol{u} = -\boldsymbol{M}_0\Bigg(&h_1\mathrm{sig}^{1-\gamma}(\boldsymbol{z}) + h_2\mathrm{sig}^{1+\gamma}(\boldsymbol{z}) + h_3\boldsymbol{z} + \\ &\boldsymbol{F} + \frac{\hat{\theta}\boldsymbol{\eta}\boldsymbol{z}}{2\tau^2} + \frac{\hat{d}_l\boldsymbol{z}}{2\tau^2} - \ddot{\boldsymbol{q}}_d\Bigg)\end{aligned} \tag{26}$$

where $h_1 = k_1$, $h_2 = \bar{h}_2(\frac{1}{2})^{1+\frac{\gamma}{2}}$, $\bar{h}_2 = n^{\frac{\gamma}{2}}2^{\frac{\gamma}{2}}3^{\frac{\gamma}{2}}\frac{b\pi\kappa}{\gamma T_s}\sqrt{\frac{\beta_2}{\beta_1}}$, $h_3 \geq \frac{1}{2}$, $\boldsymbol{\eta} = \mathrm{diag}\{\boldsymbol{S}_1^{\mathrm{T}}\boldsymbol{S}_1, ..., \boldsymbol{S}_n^{\mathrm{T}}\boldsymbol{S}_n\} \in \Re^{n\times n}$, $\tau > 0$, $\theta = \max\{||\boldsymbol{W}_1||^2, ..., ||\boldsymbol{W}_n||^2\}$, and the fuzzy weight updating law $\hat{\theta}$ is given by

$$\dot{\hat{\theta}} = \frac{\lambda\sum_{i=1}^{n} z_i^2\boldsymbol{S}_i^{\mathrm{T}}\boldsymbol{S}_i}{2\tau^2} - m_1\hat{\theta} - c_1\hat{\theta}^{1+\gamma} \tag{27}$$

and the boundary adaptive updating law $\hat{d}_l$ is

$$\dot{\hat{d}}_l = \frac{1}{2\tau^2}||\boldsymbol{z}||^2 - m_2\hat{d}_l - c_2\hat{d}_l^{1+\gamma} \tag{28}$$

where $\lambda > 0$, $m_1 = m_2 = \left(\frac{b\pi}{\kappa\gamma T_s}\sqrt{\frac{\beta_1}{\beta_2}}\right)^{\frac{2}{2-\gamma}}$, $c_1 = \frac{3^{\frac{\gamma}{2}}\pi b\kappa(2+\gamma)}{\gamma T_s 2^{1+\frac{\gamma}{2}}\lambda^{\frac{\gamma}{2}}(1+\gamma)}\sqrt{\frac{\beta_1}{\beta_2}}$, $c_2 = \frac{3^{\frac{\gamma}{2}}\pi b\kappa(2+\gamma)}{\gamma T_s 2^{1+\frac{\gamma}{2}}(1+\gamma)}\sqrt{\frac{\beta_1}{\beta_2}}$, $\hat{\theta}$ and $\hat{d}_l$ are the estimation of θ and d_l, respectively.

Using the Young's inequality, the following inequalities hold

$$\sum_{i=1}^{n} z_i\boldsymbol{W}_i^{\mathrm{T}}\boldsymbol{S}_i \leq \frac{\theta\sum_{i=1}^{n} z_i^2\boldsymbol{S}_i^{\mathrm{T}}\boldsymbol{S}_i}{2\tau^2} + \frac{n\tau^2}{2} \tag{29}$$

$$\begin{aligned}\boldsymbol{z}^{\mathrm{T}}\boldsymbol{D}' \leq&\frac{||\boldsymbol{z}||^2}{2\tau^2}d_a^2 + \frac{\tau^2}{2}\\ =&\frac{||\boldsymbol{z}||^2}{2\tau^2}d_l + \frac{\tau^2}{2}\end{aligned} \tag{30}$$

where $d_l = d_a^2$.

Substituting (26), (29) and (30) into (25) yields

$$\begin{aligned}\dot{V}_2 \leq&\dot{V}_1 + \frac{\tilde{\theta}\sum_{i=1}^{n} z_i^2\boldsymbol{S}_i^{\mathrm{T}}\boldsymbol{S}_i}{2\tau^2} + \frac{n\tau^2}{2} + \frac{||\boldsymbol{z}||^2}{2\tau^2}\tilde{d}_l + \frac{\tau^2}{2} -\\ &h_1(||\boldsymbol{z}||^2)^{1-\frac{\gamma}{2}} - n^{-\frac{\gamma}{2}}h_2(||\boldsymbol{z}||^2)^{1+\frac{\gamma}{2}} - h_3||\boldsymbol{z}||^2\\ \leq&-\bar{k}_1V_2^{1-\frac{\gamma}{2}} - \bar{h}_2n^{-\frac{\gamma}{2}}2^{-\frac{\gamma}{2}}V_2^{1+\frac{\gamma}{2}} + \frac{\tilde{\theta}\sum_{i=1}^{n} z_i^2\boldsymbol{S}_i^{\mathrm{T}}\boldsymbol{S}_i}{2\tau^2}\\ &+\frac{\tilde{d}_l||\boldsymbol{z}||^2}{2\tau^2} + \vartheta_1\end{aligned} \tag{31}$$

where $\tilde{\theta} = \theta - \hat{\theta}$, and $\vartheta_1 = 0.2785n\varpi + \frac{n+1}{2}\tau^2$.

3.2 Stability Analysis

Theorem 1 *Consider the robotic manipulator system (1) in the presence of external disturbances and model uncertainties. With the virtual controller (15), predefined-time controller (26), and adaptive update laws (27) and (28), the tracking error $\boldsymbol{e}$ can converge to a sufficiently small region around the origin within the predefined time T_s.*

Proof 1 *Choose the positive Lyapunov function as*

$$V_3 = V_2 + \frac{1}{2\lambda}\tilde{\theta}^2 + \frac{1}{2}\tilde{d}_l^2. \tag{32}$$

Differentiating (32) yields

$$\begin{aligned}\dot{V}_3 =&\dot{V}_2 - \frac{1}{\beta}\tilde{\theta}\dot{\hat{\theta}} - \tilde{d}_l\dot{\hat{d}}_l\\ \leq&-\bar{k}_1V_2^{1-\frac{\gamma}{2}} - \bar{h}_2n^{-\frac{\gamma}{2}}2^{-\frac{\gamma}{2}}V_2^{1+\frac{\gamma}{2}} + \vartheta_1 +\\ &\tilde{\theta}\left(\frac{\sum_{i=1}^{n} z_i^2\boldsymbol{S}_i^{\mathrm{T}}\boldsymbol{S}_i}{2\tau^2} - \frac{1}{\lambda}\dot{\hat{\theta}}\right) + \tilde{d}_l\left(\frac{||\boldsymbol{z}||^2}{2\tau^2} - \dot{\hat{d}}_l\right).\end{aligned} \tag{33}$$

Substituting (27) and (28) into (33) leads to

$$\dot{V}_3 \leq -\bar{k}_1 V_2^{1-\frac{\gamma}{2}} - \bar{h}_2 n^{-\frac{\gamma}{2}} 2^{-\frac{\gamma}{2}} V_2^{1+\frac{\gamma}{2}} + \frac{m_1}{\lambda}\tilde{\theta}\hat{\theta} + m_2\tilde{d}_l\hat{d}_l + \frac{c_1}{\lambda}\tilde{\theta}\hat{\theta}^{1+\gamma} + c_2\tilde{d}_l\hat{d}_l^{1+\gamma} + \vartheta_1. \quad (34)$$

Using the Young's inequality, one has

$$\frac{m_1}{\lambda}\tilde{\theta}\hat{\theta} = \frac{m_1}{\lambda}\tilde{\theta}(\theta - \tilde{\theta}) \leq -\frac{m_1\tilde{\theta}^2}{2\lambda} + \frac{m_1\theta^2}{2\lambda} \quad (35)$$

$$m_2\tilde{d}_l\hat{d}_l = m_2\tilde{d}_l(\theta - \tilde{d}_l) \leq -\frac{m_2\tilde{d}_l^2}{2} + \frac{m_2 d_l^2}{2}. \quad (36)$$

Substituting (35) and (36) into (34) yields

$$\dot{V}_3 \leq -\bar{k}_1 V_2^{1-\frac{\gamma}{2}} - \bar{h}_2 n^{-\frac{\gamma}{2}} 2^{-\frac{\gamma}{2}} V_2^{1+\frac{\gamma}{2}} - \frac{m_1\tilde{\theta}^2}{2\lambda} - \frac{m_2\tilde{d}_l^2}{2} + \frac{m_1\theta^2}{2\lambda} + \frac{m_2 d_l^2}{2} + \frac{c_1}{\lambda}\tilde{\theta}\hat{\theta}^{1+\gamma} + c_2\tilde{d}_l\hat{d}_l^{1+\gamma} + \vartheta_1. \quad (37)$$

According to Lemma 3, the following two inequalities hold:

$$\left(\frac{m_1\tilde{\theta}^2}{2\lambda}\right)^{1-\frac{\gamma}{2}} \leq \Theta(\gamma) + \frac{m_1\tilde{\theta}^2}{2\lambda} \quad (38)$$

$$\left(\frac{m_2\tilde{d}_l^2}{2}\right)^{1-\frac{\gamma}{2}} \leq \Theta(\gamma) + \frac{m_2\tilde{d}_l^2}{2} \quad (39)$$

where $\Theta(\gamma) = (\gamma/2)\cdot\big((2-\gamma)/2\big)^{(2-\gamma)/\gamma}$.

Based on Lemma 4, one has

$$\tilde{\theta}\hat{\theta}^{1+\gamma} = \tilde{\theta}(\theta - \tilde{\theta})^{1+\gamma} \leq \frac{1+\gamma}{2+\gamma}(\theta^{2+\gamma} - \tilde{\theta}^{2+\gamma}) \quad (40)$$

$$\tilde{d}_l\hat{d}_l^{1+\gamma} = \tilde{d}_l(d_l - \tilde{d}_l)^{1+\gamma} \leq \frac{1+\gamma}{2+\gamma}(d_l^{2+\gamma} - \tilde{d}_l^{2+\gamma}). \quad (41)$$

Substituting (38)-(41) into (37), one can obtain

$$\begin{aligned}\dot{V}_3 \leq & -\bar{k}_1 V_2^{1-\frac{\gamma}{2}} - \bar{h}_2 n^{-\frac{\gamma}{2}} 2^{-\frac{\gamma}{2}} V_2^{1+\frac{\gamma}{2}} - \left(\frac{m_1\tilde{\theta}^2}{2\lambda}\right)^{1-\frac{\gamma}{2}} - \frac{2^{1+\frac{\gamma}{2}} c_1\lambda^{\frac{\gamma}{2}}(1+\gamma)}{2+\gamma}\left(\frac{\tilde{\theta}^2}{2\lambda}\right)^{1+\frac{\gamma}{2}} - \left(\frac{m_2\tilde{d}_l^2}{2}\right)^{1-\frac{\gamma}{2}} + \frac{2^{1+\frac{\gamma}{2}} c_2(1+\gamma)}{2+\gamma}\left(\frac{\tilde{d}_l^2}{2}\right)^{1+\frac{\gamma}{2}} + \vartheta_1 \\ \leq & -\frac{b\pi}{\kappa\gamma T_s\sqrt{\beta_1\beta_2}}\left(\beta_1 V_3^{1-\frac{\gamma}{2}} + \beta_2\kappa^2 V_3^{1+\frac{\gamma}{2}}\right) + \vartheta_2 \end{aligned} \quad (42)$$

where $\vartheta_2 = 2\Theta(\gamma) + m_1\theta^2/(2\lambda) + c_1(1+\gamma)\theta^{2+\gamma}/(\lambda(2+\gamma)) + m_2 d_l^2/2 + c_2(1+\gamma)d_l^{2+\gamma}/(\lambda(2+\gamma)) + \vartheta_1$.

According to Lemma 1, it is concluded from (42) that the tracking error $\boldsymbol{e}$ *can converge into a sufficiently small region*

$$\Delta = \left\{ \lim_{t\to T_s} \boldsymbol{e} \mid V_3 \leq \min\left\{ \left(\frac{b\vartheta_2\kappa\gamma T_s}{(b^2-1)\pi}\sqrt{\frac{\beta_2}{\beta_1}}\right)^{\frac{2}{2-\gamma}}, \left(\frac{b\vartheta_2\kappa\gamma T_s}{(b^2-1)\pi}\sqrt{\frac{\beta_1}{\beta_2}}\right)^{\frac{2}{2+\gamma}} \right\} \right\} \quad (43)$$

within a predefined time T_s. *The proof is completed.*

4 Simulation Results

In this section, to verify the effectiveness of the proposed control strategy, a two-link robotic manipulator is considered, in which the configuration is depicted in Figure 1.

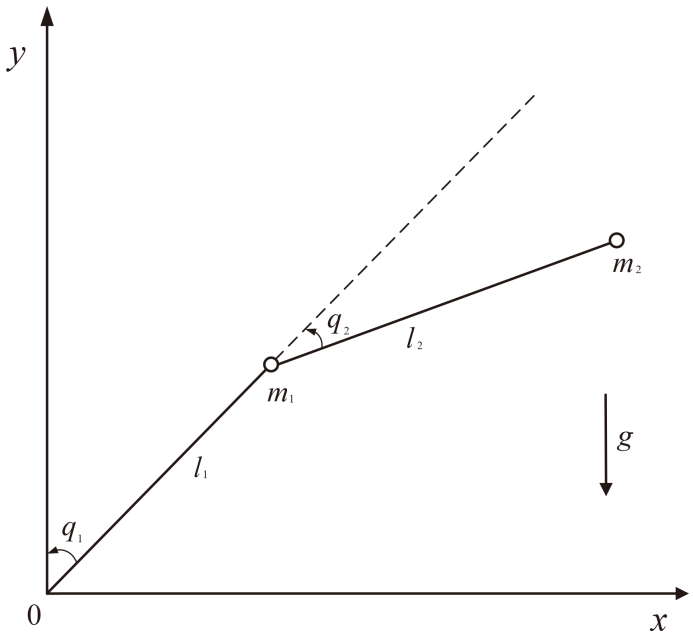

Figure 1. Configuration of a two-link robotic manipulator.

The dynamic of the two-link robotic manipulator is given by

$$\boldsymbol{M}(\boldsymbol{q}) = \begin{bmatrix} m_{11} & m_{12} \\ m_{21} & m_{22} \end{bmatrix}, \boldsymbol{C}(\boldsymbol{q},\dot{\boldsymbol{q}}) = \begin{bmatrix} c_{11} & c_{12} \\ c_{21} & c_{22} \end{bmatrix}$$
$$\boldsymbol{G}(\boldsymbol{q}) = \begin{bmatrix} g_1, & g_2 \end{bmatrix}^{\mathrm{T}}, \boldsymbol{d}(t) = \begin{bmatrix} d_1, & d_2 \end{bmatrix}^{\mathrm{T}}$$

where

$$
\begin{aligned}
m_{11} &= (m_1+m_2)l_1^2 + m_2 l_2^2 + 2m_2 l_1 l_2 \cos(q_2) + J_1,\\
m_{12} &= m_2 l_2^2 + m_2 l_1 l_2 \cos(q_2),\\
m_{21} &= m_2 l_2^2 + m_2 l_1 l_2 \cos(q_2),\\
m_{22} &= m_2 l_2^2 + J_2,\\
c_{11} &= -m_2 l_1 l_2 \sin(q_2)\dot{q}_2,\\
c_{12} &= -m_2 l_1 l_2 \sin(q_2)(\dot{q}_1+\dot{q}_2),\\
c_{21} &= m_2 l_1 l_2 \sin(q_2)\dot{q}_1,\\
c_{22} &= 0,\\
g_1 &= (m_1+m_2) l_1 g \cos(q_1) + m_2 l_2 g \cos(q_1+q_2),\\
g_2 &= m_2 l_2 g \cos(q_1+q_2).
\end{aligned}
$$

The specific parameters of the manipulator dynamic model are selected as $l_1 = 1.0$ m, $l_2 = 0.8$ m, $m_1 = 1.5$kg, $m_2 = 0.5$kg, $J_1 = 5$kg.m^2, $J_2 = 5$kg.m^2, $g = 9.8$m/s^2. The external disturbances are set as $d_1(t) = 0.5\sin(200\pi t) + 0.2\sin(t)$ N $\cdot$ m and $d_2(t) = 0.5\sin(200\pi t) + 0.2\cos(2t)$ N $\cdot$ m. The actual mass of the two links m_1 and m_2 are chosen as 1.2kg and 0.4kg, respectively. The desired trajectories are given as $q_{1d} = 1.25 - 1.4\mathrm{e}^{-t} + 0.35\mathrm{e}^{-4t}$ rad, and $q_{2d} = 1.25 + \mathrm{e}^{-t} - 0.25\,\mathrm{e}^{-4t}$ rad, respectively.

The parameters of virtual controller (20), predefined-time controller (26), and adaptive update laws (27) and (28) are selected as $T_s = 5$,$b = 1.5$, $\gamma = 5/13$,$\beta_1 = \beta_2 = 1$,$\tau = 2$, $\lambda = 1$,$\varpi = 0.00001$.

To verify the impact of initial conditions on the performance of the robotic manipulator system, we select three different sets of initial joint positions: $\boldsymbol{q}(0) = [0.6; 0.6]$, $\boldsymbol{q}(0) = [1; 1]$, and $\boldsymbol{q}(0) = [1.5; 1.5]$. Moreover, the initial joint velocity is set as $\dot{\boldsymbol{q}}(0) = [0.1; 0.1]$, and the tunable parameter κ is fixed as $\kappa = 0.4$.

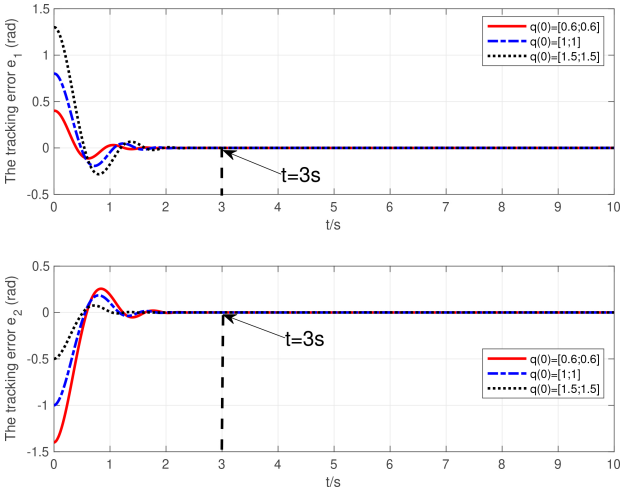

Figure 2. Tracking errors under different initial joint positions.

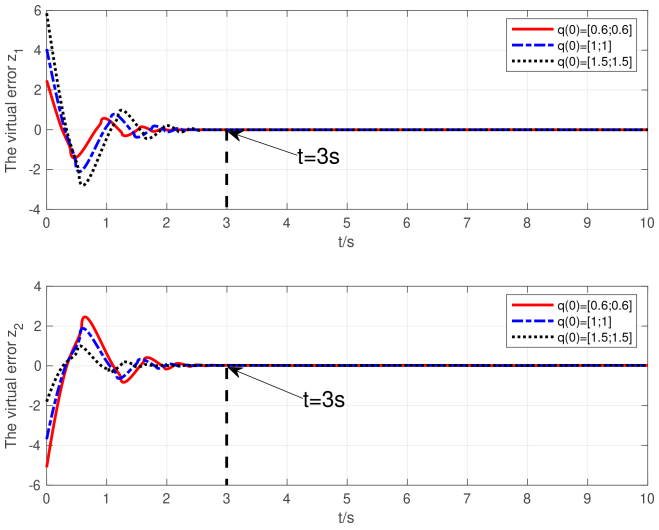

Figure 3. Virtual errors under different initial joint positions.

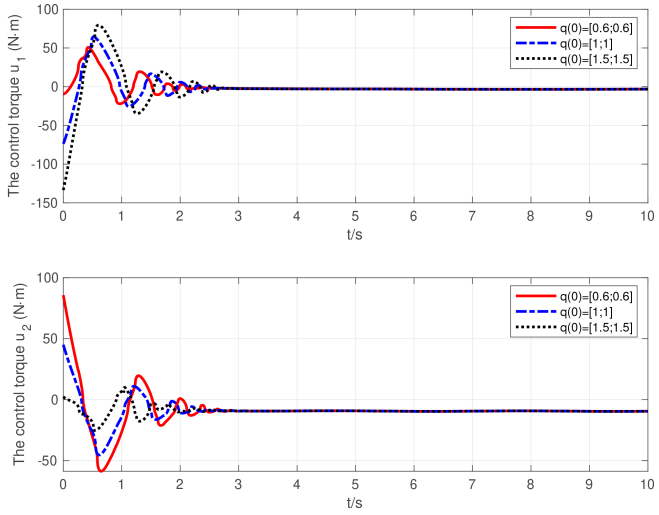

Figure 4. Control torques under different initial joint positions.

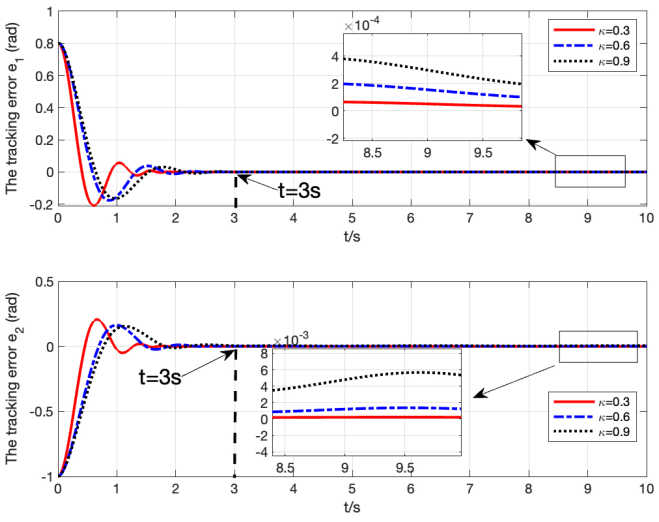

Figure 5. Tracking errors under different values of κ.

The corresponding simulation results are shown in

Figures 2-4. Figure 2 depicts the tracking errors under different initial joint positions. From Figure 2, it can be seen that the actual convergence time for the tracking errors e_1 and e_2 under different initial joint positions is 3s, which is independent of those initial positions. In addition, the actual convergence time of the tracking errors is shorter than the predefined time $T_s = 5s$, implying that the upper bound of tracking error convergence time can be precisely determined by adjusting only one control parameter. Figure 3 plots the virtual errors z_1 and z_2 under different initial joint positions. It can be observed from Figure 3 that the actual convergence time for the virtual errors z_1 and z_2 under different initial joint positions also is 3s. The control torques corresponding to the different initial joint positions are shown in Figure 4. We can conclude from Figure 4 that the greater the values of the initial joint positions, the larger the provided control torques.

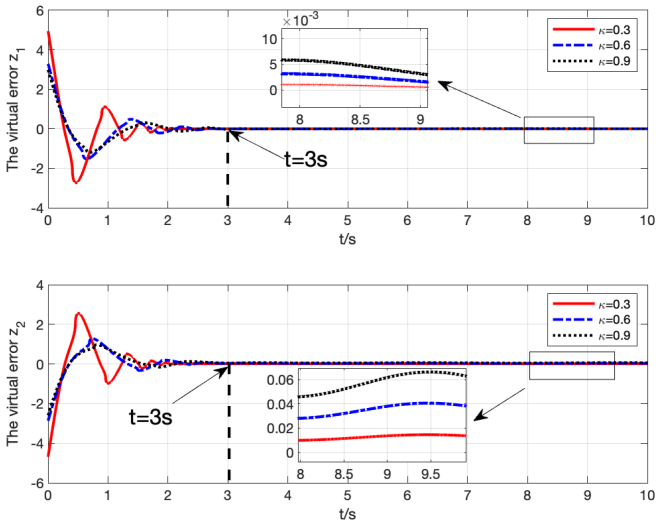

Figure 6. Virtual errors under different values of κ.

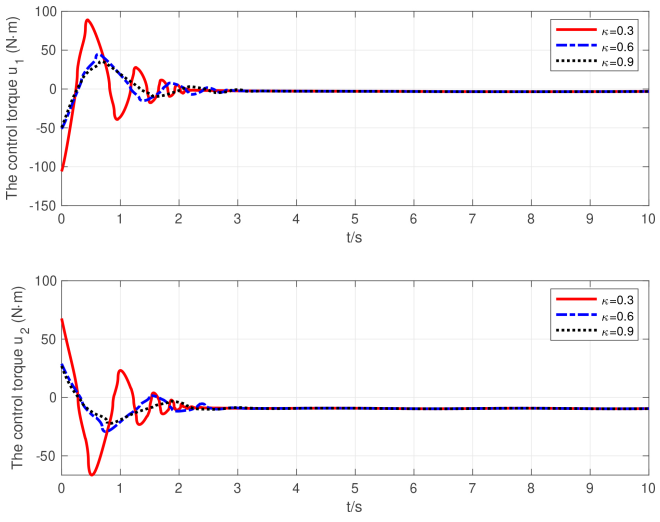

Figure 7. Control torques under different values of κ.

To assess the influence of the tunable parameter κ on the performance of the robotic manipulator system, three groups of different values of κ are selected, namely $\kappa = 0.3$, $\kappa = 0.6$, and $\kappa = 0.9$. Moreover, the initial joint position is chosen as $\boldsymbol{q}(0) = [1; 1]$. The corresponding simulation results are presented in Figures 5- 7. Figures 5 and 6 illustrate the tracking errors and virtual errors under different values of κ. From Figures 5 and 6, it is evident that the actual convergence time for both tracking and virtual errors is 3s, which is shorter than the predefined time $T_s = 5s$. Additionally, the smaller values of the parameter κ yield higher accuracy in the system's tracking and virtual errors. As shown in Figure 7, while a smaller κ facilitates faster convergence, it also results in increased control torques. Thus, selecting appropriate values for T_s and κ requires a balance between tracking performance and control torque.

5 Conclusion

This study has investigated the adaptive tunable predefined-time tracking control problem for uncertain robotic manipulators. By establishing a novel practical predefined-time stability criterion, a tunable predefined-time backstepping controller has been developed to guarantee that the bound of tracking error settling time can be explicitly determined in advance by adjusting one control parameter. The comparative simulation results validate the effectiveness and superiority of the proposed control strategy. In the future, we will focus on the predefined-time optimal tracking control problem for robotic manipulator systems, considering both tracking performance and energy costs.

Conflicts of Interest

The authors declare no conflicts of interest.

Funding

This work was supported in part by the National Natural Science Foundation of China under Grant 62203384, Grant 62222315 and Grant 62403426; in part by the Zhejiang Provincial Nature Science Foundation of China under Grant MS25F030011 and LZ22F030007.

References

[1] Yang, J., Wang, Y., Wang, T., Hu, Z., Yang, X., & Rodriguez-Andina, J. J. (2024). Time-Delay Sliding Mode Control for Trajectory Tracking of Robot Manipulators. *IEEE Transactions on Industrial Electronics*. [CrossRef]

[2] Ghodsian, N., Benfriha, K., Olabi, A., Gopinath, V., & Arnou, A. (2023). Mobile manipulators in industry 4.0: A review of developments for industrial applications. *Sensors, 23*(19), 8026. [CrossRef]

[3] Sun, M., Ge, S. S., & Mareels, I. M. (2006). Adaptive repetitive learning control of robotic manipulators without the requirement for initial repositioning. *IEEE Transactions on Robotics*, 22(3), 563-568. [CrossRef]

[4] Ding, F., Lv, L., Pan, J., Wan, X., & Jin, X. B. (2020). Two-stage gradient-based iterative estimation methods for controlled autoregressive systems using the measurement data. *International Journal of Control, Automation and Systems*, 18(4), 886-896.

[5] Ma, H., Zhang, X., Liu, Q., Ding, F., Jin, X. B., Alsaedi, A., & Hayat, T. (2020). Partially-coupled gradient-based iterative algorithms for multivariable output-error-like systems with autoregressive moving average noises. *IET Control Theory & Applications*, 14(17), 2613-2627. [CrossRef]

[6] Baek, J., Jin, M., & Han, S. (2016). A new adaptive sliding-mode control scheme for application to robot manipulators. *IEEE Transactions on industrial electronics*, 63(6), 3628-3637. [CrossRef]

[7] Dai, L., Yu, Y., Zhai, D. H., Huang, T., & Xia, Y. (2020). Robust model predictive tracking control for robot manipulators with disturbances. *IEEE Transactions on industrial electronics*, 68(5), 4288-4297. [CrossRef]

[8] Chang, W., Li, Y., & Tong, S. (2018). Adaptive fuzzy backstepping tracking control for flexible robotic manipulator. *IEEE/CAA Journal of Automatica Sinica*, 8(12), 1923-1930. [CrossRef]

[9] Yang, C., Huang, D., He, W., & Cheng, L. (2020). Neural control of robot manipulators with trajectory tracking constraints and input saturation. *IEEE Transactions on Neural Networks and Learning Systems*, 32(9), 4231-4242. [CrossRef]

[10] Zhao, K., Song, Y., Chen, C. P., & Chen, L. (2021). Adaptive asymptotic tracking with global performance for nonlinear systems with unknown control directions. *IEEE Transactions on Automatic Control, 67*(3), 1566-1573. [CrossRef]

[11] Yu, S., Yu, X., Shirinzadeh, B., & Man, Z. (2005). Continuous finite-time control for robotic manipulators with terminal sliding mode. Automatica, 41(11), 1957-1964. [CrossRef]

[12] Liu, Y., Li, H., Lu, R., Zuo, Z., & Li, X. (2022). An overview of finite/fixed-time control and its application in engineering systems. *IEEE/CAA Journal of Automatica Sinica, 9*(12), 2106-2120. [CrossRef]

[13] Zhang, Y., & Hua, C. (2022). Composite learning finite-time control of robotic systems with output constraints. *IEEE Transactions on Industrial Electronics*, 70(2), 1687-1695. [CrossRef]

[14] Gao, M., Ding, L., & Jin, X. (2021). ELM-based adaptive faster fixed-time control of robotic manipulator systems. *IEEE Transactions on Neural Networks and Learning Systems*, 34(8), 4646-4658. [CrossRef]

[15] Xie, Y., Ma, Q., Gu, J., & Zhou, G. (2022). Event-triggered fixed-time practical tracking control for flexible-joint robot. IEEE Transactions on Fuzzy Systems, 31(1), 67-76. [CrossRef]

[16] Van, M., Sun, Y., Mcllvanna, S., Nguyen, M. N., Khyam, M. O., & Ceglarek, D. (2023). Adaptive fuzzy fault tolerant control for robot manipulators with fixed-time convergence. *IEEE Transactions on Fuzzy Systems*, 31(9), 3210-3219. [CrossRef]

[17] Sánchez-Torres, J. D., Sanchez, E. N., & Loukianov, A. G. (2015, July). Predefined-time stability of dynamical systems with sliding modes. In *2015 American control conference (ACC)* (pp. 5842-5846). IEEE. [CrossRef]

[18] Hu, S., Chen, Q., Ren, X., & Wang, S. (2024). Adaptive Predefined-Time Synchronization and Tracking Control for Multimotor Driving Servo Systems. *IEEE/ASME Transactions on Mechatronics*. [CrossRef]

[19] Wang, Q., Cao, J., & Liu, H. (2022). Adaptive fuzzy control of nonlinear systems with predefined time and accuracy. IEEE Transactions on Fuzzy Systems, 30(12), 5152-5165. [CrossRef]

[20] Xie, S., & Chen, Q. (2021). Adaptive nonsingular predefined-time control for attitude stabilization of rigid spacecrafts. *IEEE Transactions on Circuits and Systems II: Express Briefs*, 69(1), 189-193. [CrossRef]

[21] Fan, Y., Yang, C., Zhan, H., & Li, Y. (2024). Neuro-Adaptive-Based Predefined-Time Smooth Control for Manipulators With Disturbance. *IEEE Transactions on Systems, Man, and Cybernetics: Systems*, 54(8), 4605-4616. [CrossRef]

[22] Jia, C., Liu, X., & Xu, J. (2023). Predefined-Time Nonsingular Sliding Mode Control and Its Application to Nonlinear Systems. IEEE Transactions on Industrial Informatics, 20(4), 5829-5837. [CrossRef]

[23] Ni, J., & Shi, P. (2020). Global predefined time and accuracy adaptive neural network control for uncertain strict-feedback systems with output constraint and dead zone. *IEEE Transactions on Systems, Man, and Cybernetics: Systems*, 51(12), 7903-7918. [CrossRef]

[24] Ding, M., Wu, H., Zheng, X., & Guo, Y. (2022). Adaptive predefined-time attitude stabilization control of space continuum robot. *IEEE Transactions on Circuits and Systems II: Express Briefs*, 71(2), 647-651. [CrossRef]

[25] Wu, Y. Y., Liu, W., Zhang, J., Li, X., & Wang, P. (2024). Tunable Predefined-Time Attitude Tracking Control for Rigid Spacecraft. *IEEE Transactions on Circuits and Systems II: Express Briefs*, 71(9), 4271-4275. [CrossRef]

[26] Munoz-Vazquez, A. J., Sánchez-Torres, J. D., Jimenez-Rodriguez, E., & Loukianov, A. G. (2019). Predefined-time robust stabilization of robotic manipulators. IEEE/ASME Transactions on Mechatronics, 24(3), 1033-1040. [CrossRef]

[27] Zhou, Q., Zhao, S., Li, H., Lu, R., & Wu, C. (2018). Adaptive neural network tracking control for robotic manipulators with dead zone. *IEEE Transactions on Neural Networks and Learning Systems*, 30(12), 3611-3620. [CrossRef]

[28] Zhu, Y., Qiao, J., & Guo, L. (2018). Adaptive sliding mode disturbance observer-based composite control with prescribed performance of space manipulators for target capturing. *IEEE Transactions on Industrial Electronics*, 66(3), 1973-1983. [CrossRef]

[29] Zou, A. M., Kumar, K. D., & de Ruiter, A. H. (2016). Robust attitude tracking control of spacecraft under control input magnitude and rate saturations. *International Journal of Robust and Nonlinear Control*, 26(4), 799-815. [CrossRef]

[30] Xie, S., Chen, Q., & Yang, Q. (2022). Adaptive fuzzy predefined-time dynamic surface control for attitude tracking of spacecraft with state constraints. *IEEE Transactions on Fuzzy Systems*, 31(7), 2292-2304. [CrossRef]

[31] Chen, Q., Li, Y., Hong, Y., & Shi, H. (2024). Prescribed-Time Robust Repetitive Learning Control for PMSM Servo Systems. *IEEE Transactions on Industrial Electronics*,71(11), 14753-14763. [CrossRef]

[32] Shi, H., Chen, Q., Hong, Y., Ou, X., & He, X. (2024). Adaptive Fuzzy Iterative Learning Control of Constrained Systems With Arbitrary Initial State Errors and Unknown Control Gain. *IEEE Transactions on Automation Science and Engineering*, 1-12. [CrossRef]

Huihui Shi received the B.E. degree in electronic engineering and automation from the Jianxing Honors College, Zhejiang University of Technology, Hangzhou, China, in 2016, and the Ph.D. degree in control science and engineering from the College of Information Engineering, Zhejiang University of Technology, in 2023.

She is currently a Post-Doctoral Researcher with Zhejiang University of Technology. Her research interests include adaptive control and iterative learning control. (Email: shidemelei@163.com)

Shuzong Xie received the M.Eng., and Ph.D. degrees in control science and engineering from the College of Information Engineering, Zhejiang University of Technology, Hangzhou, China, in 2018, and 2022, respectively.

From 2022 to 2024, he was a Postdoctoral Fellow with the Department of Control Science and Engineering, Zhejiang University, Hangzhou, China. Since 2024, he has been an Assistant Professor with the School of Automation and Electrical Engineering, Zhejiang University of Science and Technology. His current research interests include adaptive control and finite-time control with application to spacecraft attitude system and wind energy conversion system. (Email: xieshuzong@zust.edu.cn)

Qiang Chen received the B.S. degree in measure and control technology and instrumentation from Hebei Agricultural University, Baoding, China, in 2006, and the Ph.D. degree in control science and engineering from Beijing Institute of Technology, Beijing, China, in 2012.

Since 2012, he has been with the College of Information Engineering, Zhejiang University of Technology, Hangzhou, China, where he was a Professor in 2022. He has published over 100 peer-reviewed papers in journals and conference proceedings. He has been authorized more than 60 invention patents, 13 of which were transferred. His research interests include adaptive control and iterative learning control with application to motion control systems. (Email: sdnjchq@zjut.edu.cn)

Shuangyi Hu received the B.S. degree in control science and engineering from the School of Automation from Beijing Institute of Technology, Beijing, China, in 2017, and the Ph.D. degree in control science and engineering from Beijing Institute of Technology, Beijing, China, in 2023.

He is currently a Research Fellow with the College of Information Engineering, Zhejiang University of Technology, Hangzhou, China. His current research interests include adaptive control, repetitive learning control, and motor-drive servo systems. (Email: p347902@zjut.edu.cn)

Shenglun Yi received his B.Eng. in Automation from Chongqing University, China, in 2016, and his M.Sc.Eng. in Control Engineering from Beijing Technology and Business University in 2018. He earned his Ph.D. in Automation from Beijing Institute of Technology in 2022. From 2019 to 2021, he held a visiting position with Department of Information Engineering at the University of Padova.

He is currently a Researcher (Type B) in the same department at the University of Padova. His current research interests include robust estimation, information fusion, signal processing, deep learning and identification theory. (Email: shenglun@dei.unipd.it)